Landslides (2016) 13:201–210
DOI 10.1007/s10346-015-0626-x
Received: 20 October 2014
Accepted: 4 August 2015
Published online: 1 September 2015
© Springer-Verlag Berlin Heidelberg 2015

Maricar L. Rabonza · Raquel P. Felix · Alfredo Mahar Francisco A. Lagmay · Rodrigo Narod C. Eco · Iris Jill G. Ortiz · Dakila T. Aquino

Shallow landslide susceptibility mapping using high-resolution topography for areas devastated by super typhoon Haiyan

Abstract Super typhoon Haiyan, considered as one of the most powerful storms recorded in 2013, devastated the central Philippines region on 8 November 2013 with damage amounting to more than USD 2 billion. Hardest hit is the province of Leyte which is located in central Philippines. Rehabilitation of the areas that were devastated requires detailed hazard maps as a basis for well-planned reconstruction. Along with severe wind, storm surge, and flood hazard maps, detailed landslide susceptibility maps for the cities and municipalities of Leyte (7246.7 km^2) province are necessary. In order to rapidly assess and delineate areas susceptible to rainfall-induced shallow landslides, Stability INdex MAPping (SINMAP) software was used over a 5-m Interferometric Synthetic Aperture Radar (InSAR)-derived digital terrain model (DTM) grid. Topographic, soil strength, and hydrologic parameters were used for each pixel of a given DTM grid to compute for the corresponding factor of safety. The landslide maps generated using SINMAP are highly consistent with the landslide inventory derived from high-resolution satellite imagery from 2002 to 2014 with a detection percentage of 97.5 % and missing factor of 0.025. These demonstrate that SINMAP performs well despite the lack of an extensive geotechnical and hydrological database in the study area. The detailed landslide susceptibility classification is useful to identify safe and unsafe areas for reconstruction and rehabilitation efforts. These maps complement the debris flow and structurally controlled landslide hazard maps that are also being prepared for rebuilding Haiyan's devastated areas.

Keywords Landslide · Natural hazard · SINMAP · Susceptibility map · Spatial analyses · Philippines

Introduction

On 8 November 2013, typhoon Haiyan (Typhoon "Yolanda" in the Philippines) reached its peak intensity and swept through the central Philippines with 1-min sustained winds of 315 km/h at 1800 UTC (JTWC 2013). Powerful winds, heavy rains, and storm surges triggered widespread flooding and landslides, particularly affecting the provinces of Leyte (Fig. 1). Typhoon Haiyan left 6300 fatalities, 28,689 injured, and 1061 missing, as well as damage amounting to over USD 2 billion (NDRRMC 2014).

Although strong winds and storm surges of up to 5–6 m (Lagmay et al. 2015) were the primary causes of damage in Leyte, landslides were also a significant factor. Shallow landslides are rapid downhill flows of rocks and mud—typically induced by heavy rainfall—with speeds exceeding 55 km/h (Hong et al. 2007). They constitute one of the most significant hazards in complex terrain exposed to frequent heavy rainfall (Liao et al. 2010). Relevant shallow landslide-controlling factors include local conditions such as slope materials and slope surface morphology, soil properties, topography, groundwater, lithology, bedrock permeability, and land cover (D'Amato Avanzi et al. 2004; Hong et al. 2007; Liao et al 2010; Wieczorek and Sarmiento 1988). Usually, the triggering mechanism for shallow landslides on destabilized slopes usually begins with excessive rainfall. It is characterized by infiltration into the soil leading to the buildup of pore pressure, reduced soil suction value, reduced shear strength, and increased shear stress, weakening slope stability (Antronico and Gullà 2000; Campus et al. 2001; D'Amato Avanzi et al. 2003; Giannecchini 2006; Van Asch et al. 1999). This could cause surface sliding due to the textural-granulometric discontinuity within the soil-bedrock interface, causing drastic changes in the infiltration rate (Wieczorek 1987). Slope instability brought about by the complex interaction of interrelated factors becomes a major concern when they lie in close proximity to people and property (Soeters and Van Westen 1996).

Conventionally, landslide susceptibility assessments are conducted through field surveys to account for multiple relevant controlling factors (Hong et al. 2007). However, the zonation of shallow landslide potential for provinces with large areas may be difficult in the Philippines, especially given the difficulty of accessing mountainous areas and the cost of ground monitoring networks. Thus, remote sensing may be the only practical means to obtain data for landslide susceptibility mapping (Catani et al. 2005; Hong et al. 2007; Nadim et al. 2006). High-resolution satellite remote sensing products can provide detailed provincial-wide shallow landslide susceptibility maps. Studies conducted by Fabbri et al. (2003) show that the layers extracted solely from a digital elevation model (DEM) generated more accurate results than layers derived from geological data, surficial materials, and land use, indicating that topography is the primary determinant of landslide location (Coe et al. 2004; Hong et al. 2007).

It is also important to develop accurate hazard maps pinpointing the locations of areas vulnerable to landslides for rehabilitation work. The identification of potential landslides and the delineation of unstable and suitable areas for development can help ensure public safety through improved land use and disaster management planning, management of residential and recreational areas, and infrastructural development (AGS 2007; Sarkar and Kanugo 2004). In the case of areas heavily devastated by Haiyan, reliable, detailed, and readily accessible landslide susceptibility maps are critical for well-planned rehabilitation and reconstruction.

Current approach to landslide susceptibility mapping in the Philippines

Prior to this work, government agencies in the Philippines implement a qualitative method for landslide susceptibility mapping. This involves the use of landslide inventories, geologic maps, and geomorphologic information to identify possible sites of failure.

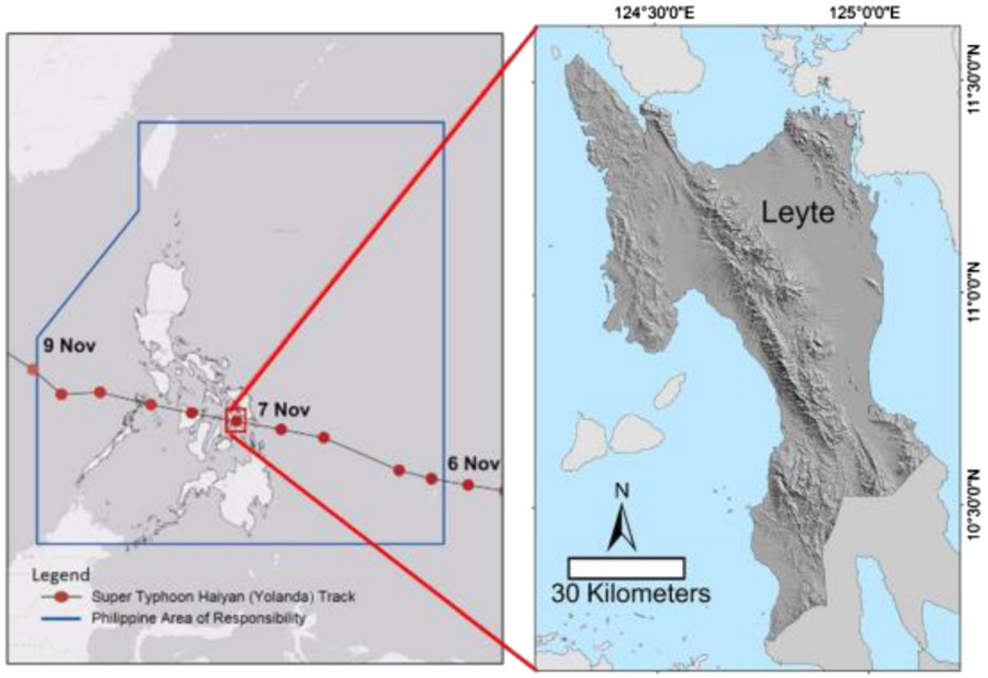

Fig. 1 Track of super typhoon Haiyan across the central Philippines. The location of the study area (Leyte province) is enclosed in *red*. Typhoon track from IBTrACS (Knapp et al. 2010)

However, weights of contributing factors depend on expert opinion of specialists on the subject. The experts use a checklist to give subjective weights for the factors (e.g., slope angle, slope weight, material type, nearness to fault, degree of gully erosion, vegetative cover, presence of road cuts on hillsides, etc.) and then derive a cumulative influence factor representing the degree of hazard (Table 1). Other than the slope gradient, there are no other quantitative bases for the hazard level assigned to an area (MGB 2013). Thus, the designating weights are highly subjective.

To date, quantitative and deterministic methods for landslide susceptibility assessment has not been used on a nationwide scale in the Philippines. The recent availability of high-resolution topographic models for the country has made this possible. Quantitative procedures are advantageous in rehabilitation purposes wherein rapid assessment is highly critical to conduct well-planned reconstruction and rehabilitation.

A sample of maps made by Mines and Geosciences Bureau - Department of Environment and Natural Resources (MGB-DENR) Philippines is shown in Fig. 2. These belong to the current national maps for landslide susceptibility. In the context of disaster management, hazard maps of 1:100,000 to 1:50,000 are not suitable for localized emergency response. Current enhancement efforts by the MGB include producing hazard maps at a finer scale of 1:10,000 (Fig. 2b).

The same scenario occurs in all the available susceptibility maps in the country. The major goal is to improve these existing government maps of the Philippines to enhance post-disaster rehabilitation using newly available high-resolution terrain data and landslide information. It is also imperative to expand options

Table 1 Landslide susceptibility parameters currently used MGB-DENR—Philippines to determine the landslide hazard susceptibility of a given area (MGB 2013)

Landslide susceptibility parameters	Low	Moderate	High	Very high
Slope gradient	Low to moderate (<18°)	Moderate to steep (18°–35°)	Steep to very steep (>35°)	Steep to very steep (>35°)
Weathering/soil characteristics	Slight to moderate	Moderate	Intense; soil usually non-cohesive	Intense; soil usually non-cohesive
Rock mass strength	Very good to good	Fair	Poor to very poor	Poor to very poor
Ground stability	Stable with no identified landslide scars, either old, recent, or active	Soil creep and other indications for possible landslide occurrence are present.	Inactive landslides evident; tension cracks present	Active landslides evident; tension cracks, bulges, terracettes, seepage present
Human-initiated effects				May be an aggravating factor

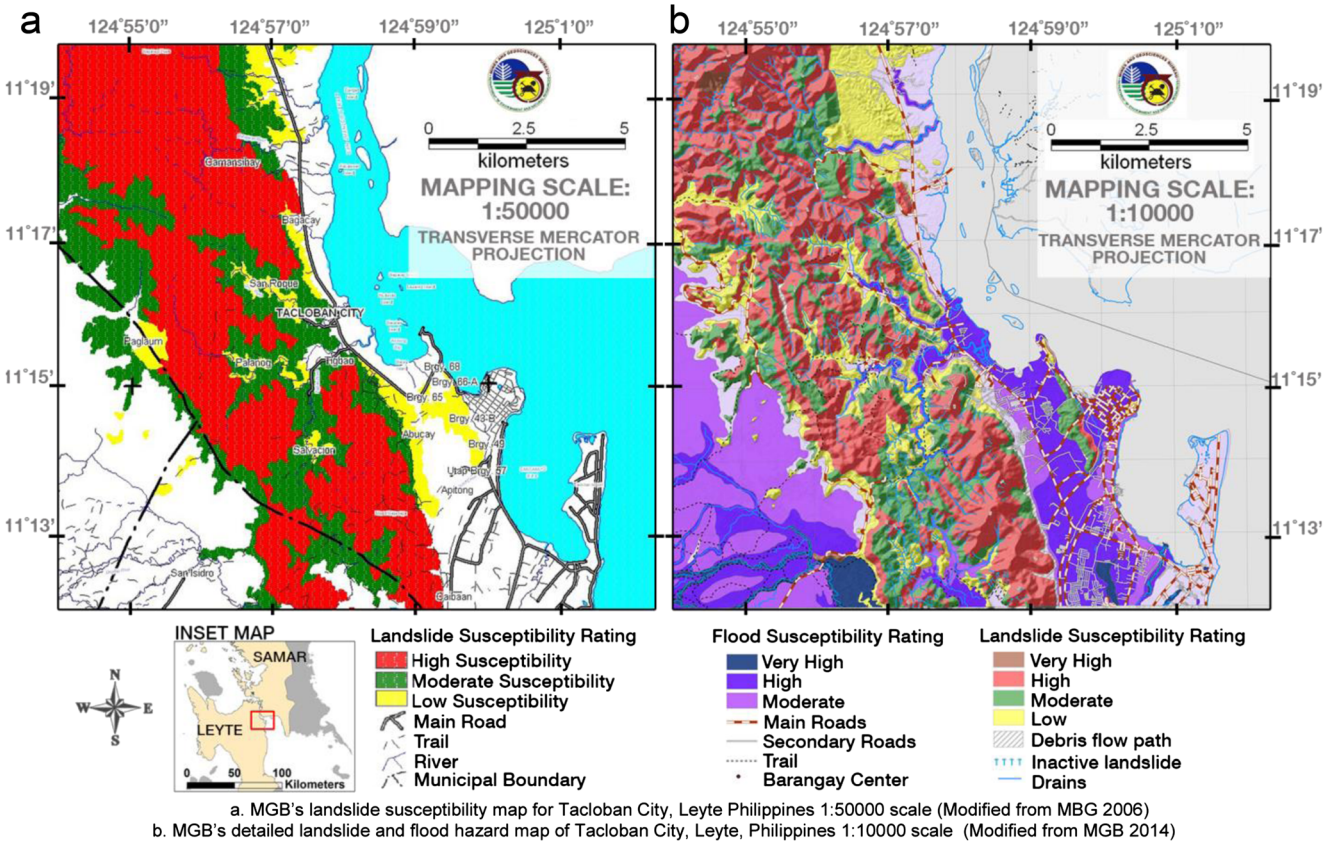

a. MGB's landslide susceptibility map for Tacloban City, Leyte Philippines 1:50000 scale (Modified from MBG 2006)
b. MGB's detailed landslide and flood hazard map of Tacloban City, Leyte, Philippines 1:10000 scale (Modified from MGB 2014)

Fig. 2 **a** MGB's landslide susceptibility map for Tacloban City, Leyte, Philippines, 1:50000 scale (modified from MGB 2006). **b** MGB's detailed landslide and flood hazard map of Tacloban City, Leyte, Philippines, 1:10000 scale (modified from MGB 2014)

of evacuation and relocation to prevent repeat of disasters within the area in the future.

Here, we implement a widely used method to characterize shallow landslides that can be employed in the nationwide mapping effort as a rapid shallow landslide assessment method. Using the typhoon- and landslide-prone Leyte province as a case study, available high-resolution digital elevation data is utilized to generate shallow landslide susceptibility maps. Unlike delineating hazard zones using historical data, maps generated using a deterministic slope stability geographic information system (GIS) model incorporates pixel-specific soil strength parameters and hydraulic characteristics. Also, it takes full advantage of the fact that landslide source areas are, in general, strongly controlled by shallow groundwater flow convergence accompanied by the reduction of shear strength and increased pore water pressure (Pack et al. 2001, 2005).

The most recent approaches to deterministic slope stability research involves diverse hydrology models using geotechnics at different levels of complexity (Connell et al. 2001; Dietrich et al. 1992, 1993, 1995, 2001; Grayson et al. 1992a, b; Lan et al. 2004; Montgomery and Dietrich 1994; Pack et al. 1998, 2001, 2005; Wu and Sidle 1995). Successful physically based stability model examples are SHALSTAB (shallow slope stability model; Montgomery and Dietrich 1994), SINMAP (Stability Index Mapping; Pack et al. 2005; Tarboton 1997), TRIGRS (Transient Rainfall Infiltration and Grid-Based Regional Slope-Stability Model; Baum et al. 2008), and SLIP (Shallow Landslide Instability Prediction; Montrasio 2000; Montrasio and Valentino 2008). Other examples of advanced hydrology models that involve modelling of groundwater and vadose zone flows are GEOtop-FS (Rigon et al. 2006), TOPMODEL (Beven and Kirkby 1979), dSLAM (Wu and Sidle 1995), and SHETRAN (Burton and Bathurst 1998). SINMAP has been widely used and tested in several landslide-prone areas because of its applicability, minimum requirement for input while allowing multi-calibration of the studied area, and model modification in smaller areas (Calcaterra et al. 2004; Deb and El-Kadi 2009; Lan et al. 2004; Meisina and Scarabelli 2007; Morrissey et al. 2001; Zaitchik and van Es 2003; Zaitchik et al. 2003). It also adds the capability of representing results into a probabilistic framework.

The reliability and degree of SINMAP model has been tested by Zizioli et al. (2013) by using receiver operating characteristic (ROC) analysis as compared to other widely used physically based models: SHALSTAB, TRIGRS, and SLIP. The values in the ROC curve (sensitivity against one specificity) represent the ability of a model to correctly classify between negative and positive observations. The global accuracy obtained for the SINMAP model expressed by the area under the curve (AUC) was equal to 0.79. The global accuracy for SHALSTAB, TRIGRS, and SLIP was 0.78, 0.79, and 0.78 respectively. The values demonstrate that the four models have similar degrees of success for prediction of shallow landslide source areas. Considering this, SINMAP model was selected for the case study due to limitation on geotechnical data or soil strength parameters of Leyte province. With SINMAP, the spatial variability of soil strength parameters can be expressed by a range of values.

After the SINMAP simulation, the maps were then compared to a landslide inventory derived by interpreting high-resolution satellite imagery dated 2002–2014. We then tested for accuracy and performance to determine the detection percentage (DP) and miss factor (MF) values. The shallow landslide susceptibility maps can be complemented with debris flow and structurally controlled hazard maps to identify safe and unsafe areas for disaster rehabilitation.

Methods

The Stability INdex MAPping approach to stability index modelling

The methodology (Fig. 3) involves the use of SINMAP, an ArcView GIS extension and an objective terrain stability mapping tool that combines steady-state hydrologic concepts with the infinite slope stability model and incorporates grid-based digital terrain model (DTM).

The infinite slope stability model balances the resisting components of cohesion and the destabilizing components of gravity on a failure plane parallel to the ground surface. It is applicable to shallow translational landslides controlled by shallow groundwater flow convergence. The slope stability theory does not apply to deep-seated instability (Montgomery and Dietrich 1994).

The input data required to implement the methodology include topographic slope, specific catchment area, and parameters quantifying material properties (such as soil strength) and climate (hydrologic wetness parameter). The topographic variables are computed from the DTM data. SINMAP does not require numerically precise input and accepts a range of soil strength and hydrologic values to account for uncertainty. In an approximate sense, this capability predicts landslide zones without additional input of weather data and analysis by specifying a range of values for the hydrologic wetness parameter.

Each of the input parameters is delineated on a numerical grid over the study area. The accuracy of the output is therefore heavily reliant on the accuracy of the input DTM (Pack et al. 2005).

The primary output of this modelling approach is a stability index (SI), the numerical representation of the stability of terrain and hence the probability that a pixel is stable assuming uniform distributions of parameters over the uncertainty ranges. It does not predict if shallow translational slope movements will occur, but it forecasts where they are more likely to initiate given the assumptions and input parameters used in the analysis. The indices are not to be interpreted as numerically precise and are most appropriately interpreted as indications of *relative shallow landslide susceptibility*. SI values range between 0 (most unstable) and 1 (least unstable) (Pack et al. 2001).

The selection of breakpoints of stability index values is subjective. For mapping purposes in the Philippines, three major susceptibility ratings are used for shallow landslide susceptibility maps: high ($1.0 \geq SI > 0$), moderate ($1.25 \geq SI > 1.0$), and low ($1.5 \geq SI > 1.25$). Stability index values greater than 1.5 are classified as stable zones. Moreover, SI less than 0 classify regions where the slope is held in place by forces not represented in the model (e.g., bedrock outcrops, man-made slope protection).

SINMAP uses the following formula to calculate the stability index based on the infinite slope equation proposed by Hammond et al. (1992).

$$FS = \frac{C + \cos\theta\left[1 - \min\left(\frac{R}{T}\frac{a}{\sin\theta}, 1\right) r\right]\tan\phi}{\sin\theta} \quad (1)$$

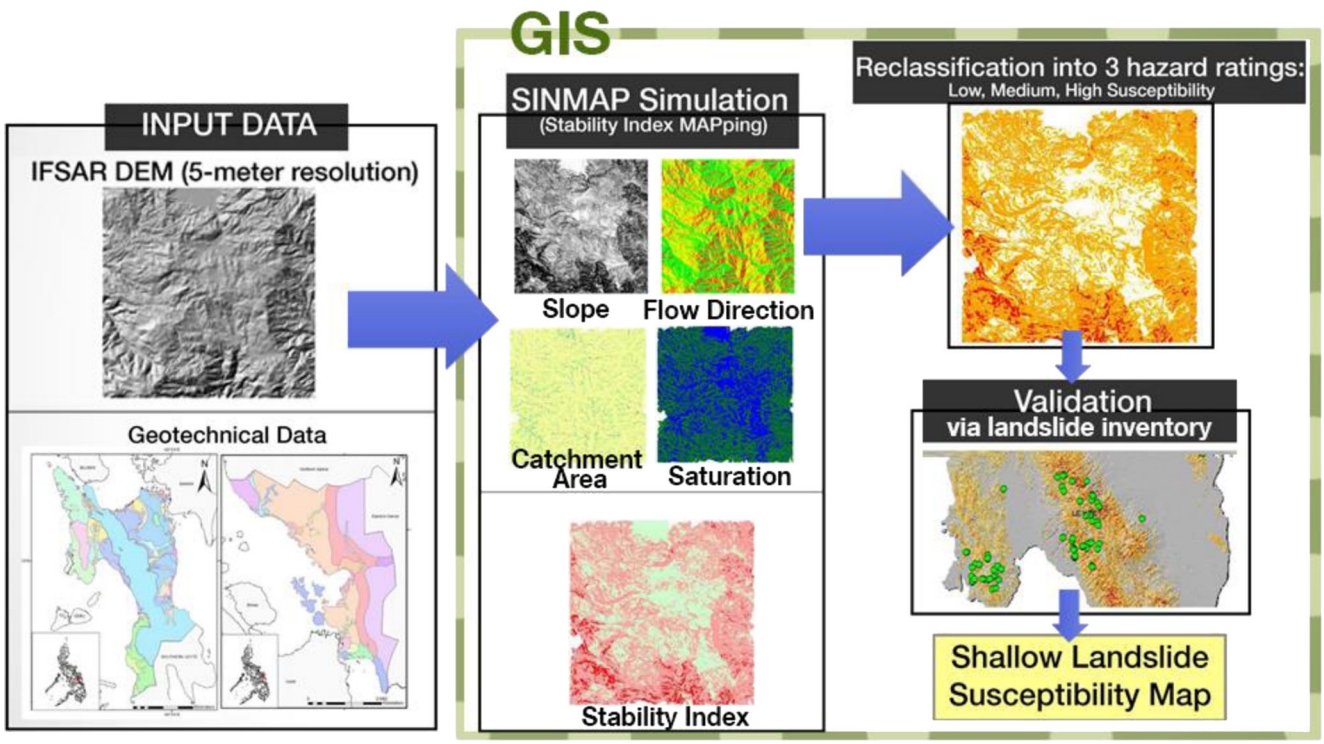

Fig. 3 Process flow of shallow landslide susceptibility mapping using SINMAP

where

FS	Factor of safety
a	Topographic catchment area
C	Dimensionless cohesion=$(Cr+Cs)=h\rho_s g$
C_r	Root cohesion
C_s	Soil cohesion
h	Soil thickness
ρ	Soil density
g	Gravity constant
hw	Height of water
R	Recharge
r	Water density (ρ_w) to soil density (ρ_s) ratio
T	Soil transmissivity=soil hydraulic conductivity×h
ϕ	Soil internal angle of friction
θ	Slope

The variables θ and a are obtained from the DTM topography. Other parameters, C (cohesion), ϕ (soil angle of friction), T/R (transmissivity divided by recharge), and r (the ratio of water and soil density) are manually entered into the model. These are the more uncertain parameters and are set in terms of lower and upper bound values. The smallest C and tan phi together with the largest R/T define the most conservative (worst case) scenario within the assumed variability in the input parameters (Pack et al. 2001).

Soil data of the study areas

Leyte province has an extensive cover of clay soil (Fig. 4). Clay loam and sand are also present but cover only relatively smaller portions of Leyte. The soil type at most mountainous areas are undifferentiated.

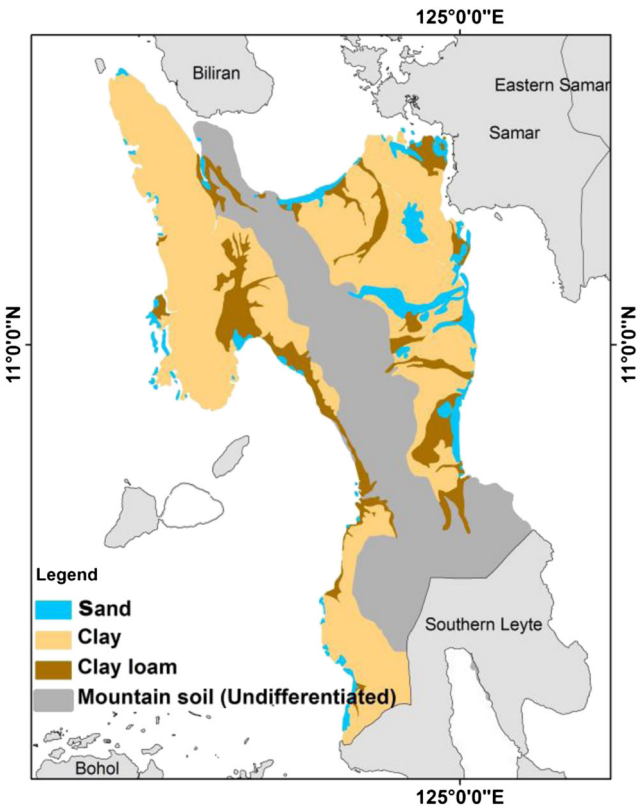

Fig. 4 Leyte soil map (digitized from BSWM 2014)

Digital terrain model grid data

The study used an Interferometric Synthetic Aperture Radar (InSAR)-derived DTM of Leyte provided by the National Mapping and Resource Information Authority (NAMRIA).

InSAR-derived products can be obtained from airborne surveys using single-pass systems or from space-borne satellite platforms using single- and repeat-pass systems (Dowman 2004). This technique is used to generate a high-resolution DEM suited for broad survey coverage. There are two types of DEM products: the digital surface model (DSM) and the DTM. The former is derived directly from the survey and represents the actual earth surface which includes vegetation and infrastructure. The DTM is produced by removing the vegetation and buildings from the DSM using filtering algorithms leaving only a representation of the actual terrain (Dowman 2004).

The raw data is acquired using Intermap's STAR-3 InSAR system that includes an X-band InSAR mounted on Learjet 36A aircraft at a flight height of 4–12 km above mean sea level and a baseline tilt angle of 1.3°. One of the obtained raw data from the survey is the DSMs. These are processed to generate DTMs with a 5-m spatial resolutions and 2- and 1-m horizontal and vertical accuracy, respectively (NAMRIA 2013) The projection datum used is the Philippine Reference System of 1992 (PRS92) which is based on the World Geodetic System of 1984 (WGS84) (Floris et al. 2010; Geospatial 2011).

Geotechnical data

Parameters not determined by the DTM such as soil strength, cohesion, angle of friction, transmissivity, and hydraulic conductivity are considered more uncertain and are specified in terms of upper and lower boundary values (Pack et al. 2001). The calibration parameters used for the simulation encompasses the typical soil parameter values for clay and clay loam, which are the dominant soil types in Leyte province (Table 2).

The equation used to determine the dimensionless cohesion combines root and soil cohesion. Theoretically, this is the ratio of the cohesive strength of the roots and soil relative to the weight of a saturated thickness of soil (Pack et al. 2005).

$$C = \frac{(C_r + C_s)}{h\rho_s g} \tag{2}$$

C_r	Root cohesion
C_s	Soil cohesion
h	Soil thickness
ρ_s	Soil density
g	Acceleration due to gravity

Internal angle of friction is a measure of the shear strength of soil due to friction determined in the laboratory using direct shear strength or triaxial stress test.

The effective recharge rates used in this study have been derived from lower and upper precipitation limits (i.e., 50 and 200 mm/day). A 50-mm/day rain rate was chosen as a minimum rate and 200 mm/day was used as the maximum (i.e., an extreme

Table 2 Soil calibration parameters for SINMAP simulation

	Soil density (kg/m^3)	Cohesion		Internal angle of friction		Approximate T/R	
		Min	Max	Min	Max	Min	Max
Clay to clay loam	1900	0	0.8	25	35	20	200

example of the precipitation that can produce shallow translational movement). This range matches the maximum accumulated rainfall of 440 mm for a 72-h period or 147 mm/day on average (MapAction 2013).

The transmissivity rate (m^2/h) was calculated using the equation, $T=Kb$, where K is the hydraulic conductivity of the soil and b is the soil depth in meters. In the context of shallow landslide movement, soil thickness of 1.5 m is assumed to be uniform in the simulation. Data on hydraulic conductivity is obtained from a database of soils in the Philippines (Hamazaki et al. 1990). Field and laboratory descriptions and test results, along with literature values for soil properties given in Hammond et al. (1992) were also used to constrain reasonable ranges of soil input parameters for the stability index modelling.

Validation

The validation process of the generated SINMAP model is summarized on Fig. 5. Landslide inventory map consisting of 363 landslides was used to validate the SINMAP model for Leyte province. The inventory utilized remote sensing techniques using various satellite images that have imagery dates from 2002 to 2014. Satellite imagery includes SPOT of 5 to 10 m spatial resolution, QuickBird of 0.6 to 2.4 m, and WorldView of 0.5 m. These images were inspected using manual detection method to identify landslide events in Google Earth, freeware program, depending on its availability.

Satellite images were loaded and inspected in Google Earth. Detected landslide events were delineated with polygons by outlining the visible disturbed body. Each identified landslide was classified based on Cruden and Varnes classification (Varnes 1958, 1978). The types of landslides indentified were mainly slides and flows. The assigned polygons were saved as vector files and analyzed in ArcGIS. The landslide inventory statistics including number of landslide, total surface area damage, and density per locality were computed using the satellite images of Leyte province.

Visual comparison was done with the SINMAP model and the landslide inventory. Accuracy assessment is performed by calculation of detection percentage and miss factor.

Results

Visual comparison of model and landslide inventory

The area distribution for low, medium, and high susceptibility to shallow landslides generated by SINMAP is shown in Fig. 6a. Unsafe areas from shallow landslides were found to be 31 % of the total land area of Leyte. Safe areas from shallow landslides comprise 69 %. The previous 1:10,000 landslide susceptibility map by MGB (Fig. 2b) presents noticeably less stable areas compared to the SINMAP model (54 %) as shown in Fig. 6b.

Initially, visual comparison was done by manual overlaying of the landslide inventory over the SINMAP model and MGB map. The number of landslide polygons that fall within each susceptibility class is tabulated (Tables 3 and 4). Among the 363 landslide polygons in Leyte, 9 were within the stable zones of the SINMAP model (Table 3). Majority of the polygons fell within the medium (66.1 %) susceptibility zones. For the MGB map, most polygons fell within the high and very high susceptibility zones (Table 4).

Accuracy assessment

The number and extent of mapped landslides are critical to disaster relief and deterministic landslide assessment (Yange et al. 2013). Therefore, in this procedure, the susceptibility zones defined

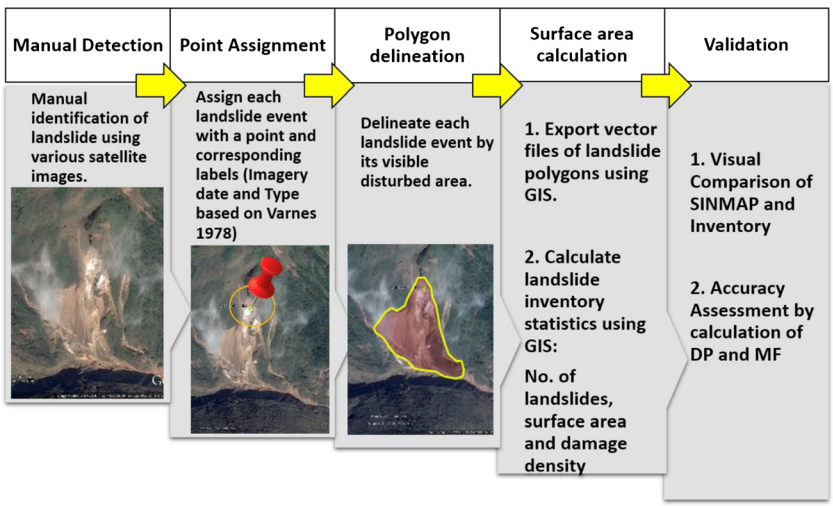

Fig. 5 Process flow of validation of SINMAP model

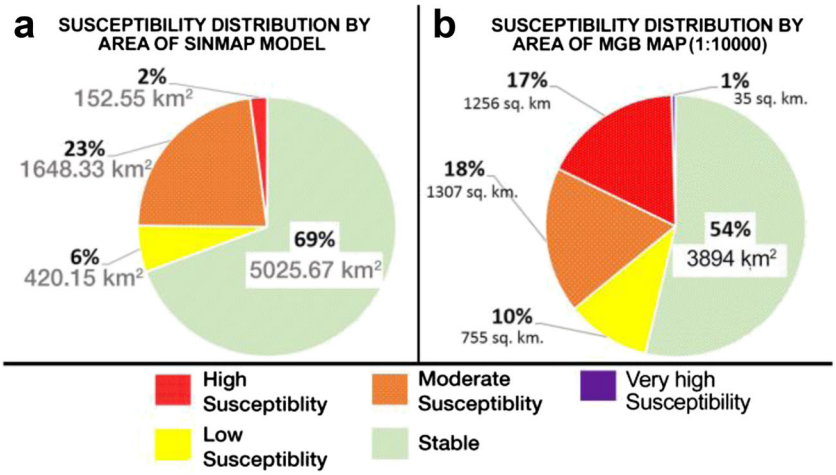

Fig. 6 Distribution of landslide susceptibility by area in Leyte province generated by SINMAP (**a**) and MGB (**b**)

by the SINMAP model were compared with the manually delineated landslide inventory. This accuracy assessment procedure is also done to the MGB map to compare its accuracy with the SINMAP model.

By visual comparison, the landslide polygons were either marked as true positive or false negative using the following category definitions:

- True positive (TP): a landslide event occurred at the area of instability defined by SINMAP
- False negative (FN): a landslide event occurred *outside* the area of instability defined by SINMAP

Once the number of landslide polygons belonging to each susceptibility category is determined, the performance of the SINMAP model for Leyte was evaluated using the following statistical measures:

$$MF = FN/TP \tag{3}$$

$$DP = 100 \times \frac{TP}{TP + FN} \tag{4}$$

The *miss factor* (*MF*) is a measure of omission error where the SINMAP model defined actual landslide areas as stable. The *detection percentage* (*DP*) is the percentage of landslide areas correctly classified by the SINMAP model as unstable (Lee et al. 2003; Shufelt 1999).

The 354 polygons captured by the SINMAP model were considered as TP, whereas the 9 landslide polygons outside the model were considered as FN. For the MGB map, 351 polygons are captured (TP) and 12 are outside the susceptibility zones (FN).

The SINMAP results showed that the DP for the study area was 97.5 % with MF of 0.025. These values demonstrate that the SINMAP approach performs well despite the lack of an extensive geotechnical and hydrological database in the study area. This also suggests a consistency in the accuracy of the InSAR-derived DTM and the high-resolution imagery used for the landslide polygon delineation. The MGB map showed a DP of 96.7 % and MF of 0.034. The accuracy of the MGB map is high which is typical for qualitative methods involving historical landslide data and relevant geomorphological information. Both susceptibility mapping methods establish high accuracy when compared to the landslide inventory; however, they differ much in the amount of stable areas they define.

Discussion

The SINMAP simulations for Leyte (Fig. 7) capture very well the landslides that have been mapped by high-resolution imagery over the span of 12 years (2002–2014). Almost all of the 363 landslides in the inventory of Leyte fall within the high (red) and moderately (orange) susceptible landslide areas. Only 2.5 % of the landslide events were not captured by the landslide susceptibility maps generated by SINMAP (Tables 3 and 4).

The stable areas identified by SINMAP within Leyte is 69 % of its total land area, 15 % more than the safe areas identified by previous landslide susceptibility map generated by the MGB (Fig. 2b) which is 54 % of the total Leyte area (Fig. 6). Nonetheless, the accuracy of the SINMAP results remain high, with the 97.5 % DP value and a MF of 0.025.

The idea of using a model that identifies landslide susceptible areas with high accuracy, and at the same time, maximizing safe and habitable areas is beneficial to the development plans of the local government. In post-disaster rehabilitation, it also expands options for siting evacuation and relocation areas. This is critical

Table 3 Summary of landslide polygons captured by SINMAP model for Leyte province

	Stable	Low	Medium	High	Total
No. of landslides	9	43	240	71	363
% of slides	2.5	11.8	66.1	19.6	100

Table 4 Summary of landslide polygons captured by MGB map for Leyte province

	Stable	Low	Medium	High–very high	Total
No. of landslides	12	0	61	290	363
% of slides	3.3	0	16.8	79.9	100

especially for the rehabilitation work of Haiyan-affected communities because it is imperative that rebuilding be carefully planned to prevent future disasters.

The landslides that were not captured by the SINMAP simulations for Leyte could be due to a different failure mechanism not considered by the infinite slope stability model. For instance, SINMAP does not consider structural controls for slope instability. These landslides occur much deeper and are controlled primarily by fracture planes that pervade in mountainous terrain. Structurally controlled landslide maps are also being prepared under the new Nationwide Hazards Mapping Program called Project NOAH where high-resolution topographic maps derived from Light Detection and Ranging (LiDAR) and InSAR are used. Along with the identification of alluvial fans and simulation of debris flows, the SINMAP and the structurally controlled landslide hazard maps will constitute the detailed hazard maps at 1:10,000 scale for landslides in Haiyan-devastated areas. These maps are available online for free in the Project NOAH portal (http://noah.dost.gov.ph).

It is critical to provide rapid assessment and delineation of areas susceptible to rainfall-induced shallow landslides for well-planned reconstruction and rehabilitation. The method of shallow landslide susceptibility mapping we implement in the Philippines addresses the need for rapidly generated landslide hazard maps. These shallow landslide hazard maps have been made freely available to different relief and rehabilitation agencies in typhoon Haiyan-ravaged areas. The shallow landslide maps that were provided are suited to the requirements of the rehabilitation and reconstruction process. It can still be and should be improved for better accuracy. More detailed geological and geotechnical assessments are necessary in the future. One area of improvement can be the replacement of InSAR-derived DTM data with more accurate LiDAR topographic data.

Conclusion

The landslide map generated using SINMAP are found to be highly accurate with DP value of 97.5 % and MF of 0.025 when compared

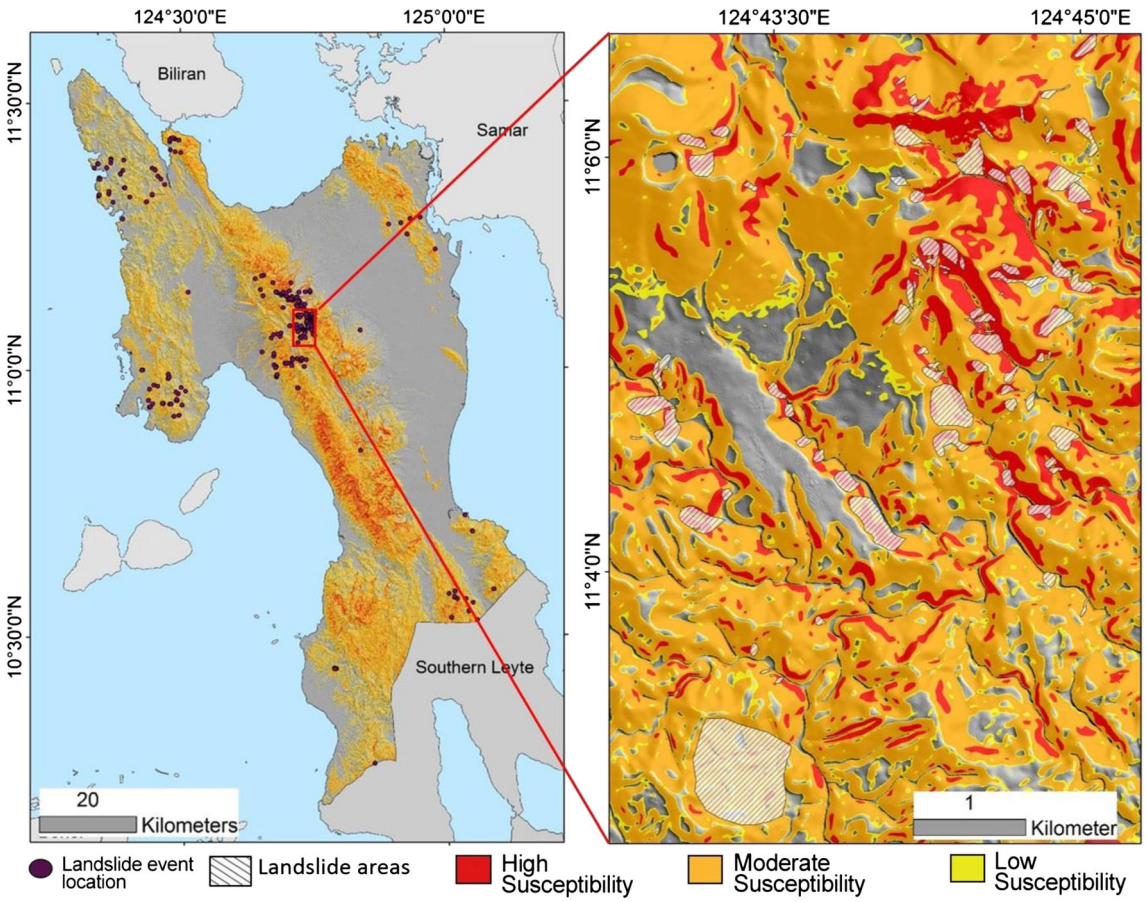

Fig. 7 Shallow landslide susceptibility map of Leyte province with a close up view in an area with identified landslides

with the landslide inventory derived from high-resolution satellite imagery for Leyte. In addition, the maps can be further improved with more detailed geological and geotechnical assessment of the study areas. Additional satellite and aerial imagery can provide more landslide inventory data to better determine the spatial extent of landslide occurrences vis-à-vis the results of the SINMAP model. The landslide susceptibility classification found in the landslide hazard maps is useful to identify unsafe and safe areas from shallow landslides. These maps complement the debris flow and structurally controlled landslide hazard maps that are also being prepared for rebuilding Haiyan-devastated areas.

Acknowledgments

The work described in this paper is supported by the Landslide Hazard Mapping Component of Project NOAH (Nationwide Operational Assessment of Hazards) under the initiatives of the Department of Science and Technology (DOST) for an improved disaster prevention and mitigation system in the Philippines. This support from the Project NOAH team is gratefully acknowledged. The authors are also grateful to the National Mapping and Resource Information Authority (NAMRIA) for providing the digital terrain model, Bureau of Soil and Water Management (BWSM) for the digitized soil maps, and the reviewers for the valuable comments.

References

AGS (2007) Guideline for landslide susceptibility, hazard, and risk zoning for land use planning. Aust Geomech 42(1):13–36

Antronico L, Gullà G (2000) Slopes affected by soil slips: validation of an evolutive model. 8th International Symposium on Landslides, Cardiff, Wales. Thomas Telford, London, pp 77–84

Baum RL, Savage WZ, Godt JW (2008) TRIGRS—a FORTRAN program for transient rainfall infiltration and grid-based regional slope stability analysis, version 2.0 US Geological Survey Open File Report 2008-1159. Reston, Virginia

Beven KJ, Kirkby MJ (1979) A physically-based variable contributing area model of basin hydrology. Hydrol Sci Bull 24(1):43–69. doi:10.1080/02626667909491834

BSWM (2014) Soil and physiography map of Leyte. Bureau of Soils and Water Management (BSWM) Map Library Platform. World Bank and Department of Agriculture. http://www.bswm.maps.da.gov.ph/maps-library. Accessed 15 August 2014

Burton A, Bathurst JC (1998) Physically-based modelling of shallow landslide sediment yield at a catchment scale. Environ Geol 35(2-3):89–99. doi:10.1007/s002540050296

Calcaterra D, de Riso R, Di Martire D (2004) Assessing shallow debris slide hazard in the Agnano Plain (Naples, Italy) using SINMAP, a physically based slope-stability model. In: Lacerda WA, Ehrlich M, Fontoura SAB, Sayao ASF (eds) 9th International Symposium on Landslides, Rio de Janeiro Brazil. Taylor and Francis Group, London, pp 177–183

Campus S, Forlati F, Sarri H, Scavia C (2001) Shallow landslides hazard assessment based on multidisciplinary studies. In: Ho KKS, Li KS (eds) 14th Southeast Asian Geotechnical Conference Hong Kong. AA Balkema, Rotterdam, pp 703–708

Catani F, Casagli N, Ermini L, Righini G, Menduni G (2005) Landslide hazard and risk mapping at catchment scale in the Arno River basin. Landslides 2(4):329–342. doi:10.1007/s10346-005-0021-0

Coe JA, Godt JW, Baum RL, Buckman RC, Michael JA (2004) Landslide susceptibility from topography in Guatemala. In: Lacerda WA, Ehrlich M, Fontoura SAB, Sayao ASF (eds) Landslides evaluation and stabilization, 10th Symposium on Landslides, Balkema Leiden. Taylor and Francis Group, London, pp 69–78

Connell LD, Jayatilaka CJ, Nathan R (2001) Modelling flow and transport in irrigation catchments: 2. Spatial application of subcatchment model. Water Resour Res 37(4):965–977. doi:10.1029/2000WR900269

D'Amato Avanzi G, Giannecchini R, Puccinelli A (2003) A contribution to an evaluation of landslide susceptibility in the Apuan Alps (Italy): geologic and geomorphic factors of 1996 soil slip-debris flows. In: Picarelli L (ed) International Conference, Fast Slope Movements: Prediction and Prevention for Risk Mitigation, Naples Italy. Patron Editore, Bologna, pp 125–130

D'Amato Avanzi G, Giannecchini R, Puccinelli A (2004) The influence of the geological and geomorphological settings on shallow landslides. An example in a temperate climate environment: the June 19, 1996 event in northwestern Tuscany (Italy). Eng Geol 73(3-4):215–228. doi:10.1016/j.enggeo.2004.01.005

Deb SK, El-Kadi AI (2009) Susceptibility assessment of shallow landslides on Oahu, Hawaii, under extreme-rainfall events. Geomorphology 108(3-4):219–233. doi:10.1016/j.geomorph.2009.01.009

Dietrich WE, Wilson CJ, Montgomery DR, McKean J, Bauer R (1992) Erosion thresholds and land surface morphology. J Geol 20(8):675–679. doi:10.1130/0091-7613(1992)020<0675:ETALSM>2.3.CO;2

Dietrich WE, Wilson CJ, Montgomery DR, McKean J (1993) Analysis of erosion thresholds, channel networks, and landscape morphology using a digital terrain model. J Geol 101:259–278

Dietrich WE, Reiss R, Hsu M, Montgomery DR (1995) A process-based model for colluvial soil depth and shallow landsliding using digital elevation data. Hydrol Process 9:383–400

Dietrich WE, Bellugi D, Real De Asua R (2001) Validation of shallow landslide model, SHALTAB, for forest management. In: Wigmosta MS, Burges SJ (eds) Land use and watersheds: human influence on hydrology and geomorphology in urban and forest areas. American Geophysical Union, pp 195-227

Dowman I (2004) Integration of Lidar and IfSAR for mapping. Int Arch Photogramm Remote Sens, Istanbul, Turk 35(B2):90–100

Fabbri AG, Chung CF, Cendrero A, Remondo J (2003) Is prediction of future landslides possible with a GIS? Nat Hazards 30(3):487–503. doi:10.1023/B:NHAZ.0000007282.62071.75

Floris M, Squarzoni C, Hundseder C, Mason M, Genevois R (2010) The use of IfSAR data in GIS-based landslide susceptibility evaluation. Geophys Res Abstr 12

Geospatial World (2011) PRS92 surveying standard compulsory in the Philippines. Geospatial World. http://geospatialworld.net/News/View.aspx?id=21573_Article. Accessed 29 May 2015

Giannecchini R (2006) Relationship between rainfall and shallow landslides in the southern Apuan Alps (Italy). Nat Hazards Earth Syst Sci 6:357–364. doi:10.5194/nhess-6-357-2006

Grayson RB, Moore ID, McMahon TA (1992a) Physically based hydrologic modelling: 1. A terrain-based model for investigative purposes. Water Resour Res 28(10):2639–2658. doi:10.1029/92WR01258

Grayson RB, Moore ID, McMahon TA (1992b) Physically-based hydrologic modelling: 2. Is the concept realistic? Water Resour Res 28(10):2659–2666. doi:10.1029/92WR01259

Hamazaki T, Paningbatan EP Jr, Pampolino MF (1990) Data base on red-yellow and related soils in the Philippines: Part 2 Visayas and Mindanao soils. Technical Paper at College of Agriculture. University of the Philippines Los Baños and Tropical Agriculture Research Center, Tokyo

Hammond C, Hall D, Miller S, Swetik P (1992) Level I stability analysis (LISA) documentation for Version 2.0: General Technical Report INT-285. USDA Forest Service, Intermountain Research Station

Hong Y, Adler R, Huffman G (2007) Use of satellite remote sensing data in the mapping of global landslide susceptibility. Nat Hazards 43(2):245–256. doi:10.1007/s11069-006-9104-z

JTWC (2013) Joint Typhoon Warning Center Best Track Archive—Typhoon Haiyan. Naval Meteorology and Oceanography Command, Stennis Space Center, Mississippi. http://www.usno.navy.mil/JTWC/. Accessed 30 November 2013

Knapp KR, Kruk MC, Levinson DH, Diamond HJ, Neumann CJ (2010) The International Best Track Archive for Climate Stewardship (IBTrACS): unifying tropical cyclone best track data. Bull Am Meteorol Soc 91:363–376. doi:10.1175/2009BAMS2755.1

Lagmay AM, Agaton RP, Bahala MAC, Briones JBLT, Cabacaba KMC, Caro CVC, Dasallas LL, Gonzalo LAL, Ladiero CH, Lapidez JP, Mungcal MTF, Puno JVR, Ramos MMAC, Santiago J, Suarez JK, Tablazon JP (2015) Devastating storm surges of typhoon Yolanda. Int J Disaster Risk Reduct 11:1–12. doi:10.1016/j.ijdrr.2014.10.006

Lan HX, Zhou CH, Wang LJ, Zhang HY, Li RH (2004) Landslide hazard spatial analysis and prediction using GIS in the Xiaojiang watershed, Yunnan, China. Eng Geol 76(1-2):109–128. doi:10.1016/j.enggeo.2004.06.009

Lee DS, Shan J, Bethel JS (2003) Class-guided building extraction from IKONOS imagery. Photogram Eng Remote Sens 69(2):143–150

Liao Z, Hong Y, Wang J, Fukuoka H, Sassa K, Karnawati D, Fathani F (2010) Prototyping an experimental early warning system for rainfall-induced landslides in Indonesia using satellite remote sensing and geospatial datasets. Landslides 7(3):317–324. doi:10.1007/s10346-010-0219-7

MapAction (2013) Philippines typhoon Haiyan (Yolanda) accumulated rainfall 06-Nov-2013 to 09-Nov-2013. Situational data source from: PAGASA, Joint Typhoon Warning Centre Philippines. http://mapaction.org. Accessed 24 March 2014

Meisina C, Scarabelli S (2007) A comparative analysis of terrain stability models for predicting shallow landslides in colluvial soils. Geomorphology 87(3):207–223. doi:10.1016/j.geomorph.2006.03.039

MGB (2006) Landslide susceptibility map of Tacloban City quadrangle Leyte Philippines. Department of Environment and Natural Resources – Mines and Geosciences Bureau (MGB) Lands Geological Survey Division. Sheet Number 3953 I. http://gdis.denr.gov.ph/mgbpublic. Accessed 1 October 2014

MGB (2013) Guidebook for the conduct of landslide and flood susceptibility assessment and mapping (1:10000). Department of Environment and Natural Resources – Mines and Geosciences Bureau (MGB) Lands Geological Survey Division. North Avenue, Quezon City, Philippines

MGB (2014) Detailed landslide and flood hazard map of Tacloban City, Leyte, Philippines. Department of Environment and Natural Resources – Mines and Geosciences Bureau (MGB) Lands Geological Survey Division. North Avenue, Quezon City, Philippines

Montgomery D, Dietrich W (1994) A physically based model for the topographic control on shallow landsliding. Water Resour Res 30(4):1153–1171. doi:10.1029/93WR02979

Montrasio L (2000) Stability analysis of soil slip. Proc of Int Conf Risk 2000, In: Brebbia CA (ed) Wit Press, Southampton, pp 357-366

Montrasio L, Valentino R (2008) A model for triggering mechanism of shallow landslides. Nat Hazards Earth Syst Sci 8:1149–1159. doi:10.5194/nhess-8-1149-2008

Morrissey MM, Wieczorek GF, Morgan BA (2001) A comparative analysis of hazard models for predicting debris flows in Madison Country, Virginia. Open file report 01-0067. USGS (ed) US Department of the Interior, US Geological Survey, Washington

Nadim F, Kjekstad O, Peduzzi P, Herold C, Jaedicke C (2006) Global landslide and avalanche hotspots. Landslides 3(2):159–173. doi:10.1007/s10346-006-0036-1

NAMRIA (2013) The Philippine IfSAR project. Internal report jointly by NAMRIA, Intermap Technologies Inc. (Denver CO) and Certeza Infosys Corp. NAMRIA Main Office, Taguig City, Philippines

NDRRMC (2014) National Disaster Risk Reduction and Management Council (NDRRMC) Updates regarding the effects of Typhoon "Yolanda" (HAIYAN) 17 April 2014. National Disaster Risk Reduction and Management Center, Camp Aguinaldo, Quezon City, Philippines. http://www.ndrrmc.gov.ph/index.php/21-disaster-events/1329-situational-report-re-effects-of-typhoon-yolanda-haiyan. Accessed 2 June 2014

Pack RT, Tarboton DG, Goodwin CN (1998) The SINMAP approach to terrain stability mapping. In: 8th Congress of the International Association of Engineering Geology, Vancouver, British Columbia, Canada 21-25 September 1998. http://www.engineering.usu.edu/cee/faculty/dtarb/iaeg.pdf. Accessed 4 May 2013

Pack RT, Tarboton DG, Goodwin CN (2001) Assessing terrain stability in a GIS using SINMAP. In: GIS 2001. 15th annual GIS conference, Vancouver, British Columbia. http://hydrology.usu.edu/sinmap/gis2001.pdf. Accessed 4 May 2013

Pack RT, Tarboton DG, Goodwin CN, Prasad A (2005) SINMAP 2: a stability index approach to terrain stability hazard mapping technical description and users guide for version 2.0. Utah State University. http://hydrology.usu.edu/sinmap2/sinmap2.PDF. Accessed 4 May 2013

Rigon R, Bertoldi G, Over TM (2006) GEOtop: a distributed hydrological model with coupled water and energy budgets. J Hydrometeorol 7(3):371–388. doi:10.1175/JHM497.1

Sarkar S, Kanugo DP (2004) An integrated approach for landslide susceptibility mapping using remote sensing and GIS. Photogramm Eng Remote Sens 70(5):617–625

Shufelt JA (1999) Performance evaluation and analysis of monocular building extraction from aerial imagery. IEEE Trans Pattern Anal Mach Intell 21(4):311–326

Soeters R, Van Westen CJ (1996) Slope instability, recognition, analysis and zonation. In: Turner AK, Schuster RL (eds) Landslides: investigation and mitigation Special Report 247. Transportation Research Board. National Research Council. National Academy Press, Washington, pp 129–177

Tarboton DG (1997) A new method for the determination of flow direction and upslope areas in grid digital elevation models. Water Resour Res 33(2):309–319. doi:10.1029/96WR03137

Van Asch TWJ, Buma J, Van Beek LPH (1999) A view on some hydrological triggering systems in landslides. Geomorphology 30(1):25–32

Varnes DJ (1958) Landslide types and processes. In: Eckel EB (ed) Landslides and engineering practice, Special Report 29. Highway Research Board National Research Council, Washington DC, pp 20–47

Varnes DJ (1978) Slope movement types and processes. In: Schuster RL, Krizek RJ (eds) Landslides: analysis and control, Special Report 176. Transportation Research Board National Academy of Sciences, Washington DC, pp 11–33

Wieczorek GF (1987) Effect of rainfall intensity and duration on debris flows in central Santa Cruz Mountains, California. In: Costa JE, Wieczorek GF (eds) Debris flows/avalanches: processes, recognition and mitigation. Reviews in Engineering Geology, vol 7. Geological Society of America, pp 23-104

Wieczorek GF, Sarmiento J (1988) Rainfall, piezometric levels and debris flows near La Honda, California, in storms between 1975 and 1983. In: Ellen SD, Wieczorek GF (eds) Landslides, floods and marine effects of the storm of January 3-5, 1982 in the San Francisco Bay vol 1434. USGS Professional Paper, pp 43-62

Wu W, Sidle R (1995) A distributed slope stability model for steep forested basins. Water Resour Res 31:2079–2110

Yange L, Guangqi C, Bo W, Lu Z, Yingbin Z, Chuan T (2013) A new approach of combining aerial photography with satellite imagery for landslide detection. Nat Hazards 66:649–669. doi:10.1007/s11069-012-0505-x

Zaitchik BF, van Es HM (2003) Applying a GIS slope-stability model to site-specific landslide prevention in Honduras. J Soil Water Conserv 58(1):45–53

Zaitchik BF, van Es HM, Sullivan PJ (2003) Modeling slope stability in Honduras: parameter sensitivity and scale of aggregation. Soil Sci Soc Am J 67(1):268–278

Zizioli D, Meisina C, Valentino R, Montrasio L (2013) Comparison between different approaches to modelling shallow landslide susceptibility: a case history in Oltrepo Pavese, Northern Italy. Nat Hazards Earth Syst Sci 13:559–573. doi:10.5194/nhess-13-559-2013

R. P. Felix · A. M. F. Lagmay · R. N. C. Eco · I. J. G. Ortiz
National Institute of Geological Sciences,
University of the Philippines,
Diliman 1101, Quezon City, Philippines

M. L. Rabonza (✉) · R. P. Felix · A. M. F. Lagmay · R. N. C. Eco · I. J. G. Ortiz · D. T. Aquino
Nationwide Operational Assessment of Hazards, Department of Science and Technology, Quezon City, Metro Manila, NCR, Philippines
e-mail: mrabonza@noah.dost.gov.ph

R.P. Felix
email: raquel.felix@noah.dost.gov.ph

A.M.F.A. Lagmay
email: mlagmay@noah.dost.gov.ph

R.N.C. Eco
email: narod.eco@noah.dost.gov.ph

I.J.G. Ortiz
email: iris.ortiz@noah.dost.gov.ph

D.T. Aquino
email: daquino@noah.dost.gov.ph